



HAL
open science

Composition and properties of silver-containing calcium carbonate–calcium phosphate bone cement

Sylvaine Jacquart, Robin Siadous, Christel Hénocq-Pigasse, Reine Bareille,
Christine Roques, Christian Rey, Christèle Combes

► **To cite this version:**

Sylvaine Jacquart, Robin Siadous, Christel Hénocq-Pigasse, Reine Bareille, Christine Roques, et al.. Composition and properties of silver-containing calcium carbonate–calcium phosphate bone cement. *Journal of Materials Science: Materials in Medicine*, 2013, Vol. 24 (n° 12), pp. 2665-2675. 10.1007/s10856-013-5014-2 . hal-01153078

HAL Id: hal-01153078

<https://hal.science/hal-01153078>

Submitted on 19 May 2015

HAL is a multi-disciplinary open access archive for the deposit and dissemination of scientific research documents, whether they are published or not. The documents may come from teaching and research institutions in France or abroad, or from public or private research centers.

L'archive ouverte pluridisciplinaire **HAL**, est destinée au dépôt et à la diffusion de documents scientifiques de niveau recherche, publiés ou non, émanant des établissements d'enseignement et de recherche français ou étrangers, des laboratoires publics ou privés.



Open Archive TOULOUSE Archive Ouverte (OATAO)

OATAO is an open access repository that collects the work of Toulouse researchers and makes it freely available over the web where possible.

This is an author-deposited version published in : <http://oatao.univ-toulouse.fr/>
Eprints ID : 12042

To link to this article : DOI:10.1007/s10856-013-5014-2

URL : <http://dx.doi.org/10.1007/s10856-013-5014-2>

To cite this version :

Jacquart, Sylvaine and Siadous, Robin and Henocq-Pigasse, Christel and Bareille, Reine and Roques, Christine and Rey, Christian and Combes, Christèle *Composition and properties of silver-containing calcium carbonate–calcium phosphate bone cement*. (2013) *Journal of Materials Science: Materials in Medicine*, Vol. 24 (n° 12). pp. 2665-2675. ISSN 0957-4530

Any correspondence concerning this service should be sent to the repository administrator: staff-oatao@listes-diff.inp-toulouse.fr

Composition and properties of silver-containing calcium carbonate–calcium phosphate bone cement

Sylvaine Jacquart · Robin Siadous ·
Christel Henocq-Pigasse · Reine Bareille ·
Christine Roques · Christian Rey · Christèle Combes

Abstract The introduction of silver, either in the liquid phase (as silver nitrate solution: Ag(L)) or in the solid phase (as silver phosphate salt: Ag(S)) of calcium carbonate–calcium phosphate (CaCO₃–CaP) bone cement, its influence on the composition of the set cement (C-Ag(L) and C-Ag(S) cements with a Ca/Ag atomic ratio equal to 10.3) and its biological properties were investigated. The fine characterisation of the chemical setting of silver-doped and reference cements was performed using FTIR spectroscopy. We showed that the formation of apatite was enhanced from the first hours of maturation of C-Ag(L) cement in comparison with the reference cement, whereas a longer period of maturation (about 10 h) was required to observe this increase for C-Ag(S) cement, although in both cases, silver was present in the set cements mainly as silver phosphate. The role of silver nitrate on the setting chemical reaction is discussed and a chemical scheme is proposed. Antibacterial activity tests (*S. aureus* and *S. epidermidis*) and in vitro cytotoxicity

tests (human bone marrow stromal cells (HBMSC)) showed that silver-loaded CaCO₃–CaP cements had antibacterial properties (anti-adhesion and anti-biofilm formation) without a toxic effect on HBMSC cells, making C-Ag(S) cement a promising candidate for the prevention of bone implant-associated infections.

1 Introduction

The first self-setting calcium phosphate cements (CPC) were introduced in the early 1980s as biomaterials for bone repair and regeneration [1]. Since then, different CPCs have been developed; their biomimetism and their excellent osteoconductivity make them interesting candidates for dental or orthopaedic applications. On the other hand, their moulding ability allows for the optimal filling of bone. Thus, many studies have been performed in order to improve their physico-chemical properties and their biological behaviour. Nevertheless, some important issues still need to be overcome. Among them, improved resorption capability and better protection against implant-associated infections are major challenges in this field [2, 3].

Calcium carbonate–calcium phosphate (CaCO₃–CaP) mixed cements have been presented as a promising resorbable material for bone reconstruction [4]. Vaterite is a metastable polymorph of calcium carbonate whose solubility is higher than phosphocalcium apatite; a high proportion of vaterite (i.e. 50 % w/w in the solid phase) is expected to enhance the resorption of bone cement via faster physico-chemical degradation.

Different strategies have been carried out in order to prevent bacterial infection associated with the implantation of CPCs [5]. Many studies were performed on the introduction of antibiotics such as gentamicin, cephalexin or vancomycin

S. Jacquart · C. Rey · C. Combes (✉)
CIRIMAT, UPS-INPT-CNRS, ENSIACET, Université de
Toulouse, 4, allée Emile Monso, BP 44362,
31030 Toulouse Cedex 4, France
e-mail: christele.combes@ensiacet.fr

R. Siadous · R. Bareille
Inserm U1026, Bioingénierie Tissulaire, 146 rue Léo Saignat,
33076 Bordeaux Cedex, France

R. Siadous · R. Bareille
Université Bordeaux Segalen, 146 rue Léo Saignat,
33076 Bordeaux Cedex, France

C. Henocq-Pigasse · C. Roques
LGC, UMR 5503 UPS-INPT-CNRS, Faculté de Pharmacie,
Université de Toulouse, 35 chemin des Maraîchers,
31062 Toulouse Cedex 9, France

[6–10]. However, if the addition of antibiotics is well-accepted in the treatment of specific infections, it remains controversial for preventive applications because of the cost and risk of limited efficiency due to the potential resistance of bacteria to the drug [3]. The use of $\text{Ca}(\text{OH})_2$ or alkali-substituted phosphate reactants have also been proposed; the released hydroxyl ions and the formation of highly alkaline products during setting, respectively, provide an antibacterial activity [11–13]. Nevertheless, such alkaline systems raise the question of cytocompatibility and they cannot be transposed to most mineral cement, particularly acidic ones.

On the other hand, silver has been widely used in medical devices as a broad-spectrum antimicrobial agent with low toxicity [14]. In particular, an antibacterial effect was observed on *Staphylococcus aureus* (*S. aureus*), which is the most frequent infective agent after prosthesis implantation [15, 16]. It must be noted that, since the late 1970s, some cases of silver-resistant bacteria have been identified, but they remain rare and to our knowledge the main bacteria found in usual post-operative infections are not concerned [17].

Among the developed medical devices, silver was introduced by different methods into apatitic matrices during apatite synthesis, for example by co-precipitation of calcium hydroxide or calcium salt and silver nitrate with a phosphate compound, by direct formation of silver-doped hydroxyapatite (Ag-HA) coatings, or by an additional step of impregnation of the hydroxyapatite (HA) gel or HA coating in a solution of AgNO_3 [18–26].

Although silver has been frequently introduced into PMMA bone cements, only two silver-doped phosphocalcic cements have been proposed recently [27–29]. Those apatitic and brushitic cements were prepared by using silver-doped tricalcium phosphate and showed a significant reduction in the bacterial adherence of *S. aureus* and *S. epidermidis* but decreased cytocompatibility in human osteoblast cell lines.

The present study focuses on the association of silver with a CaCO_3 –CaP self-setting paste in order to confer the antibacterial activity of this cement. Two methods of introduction were investigated: the addition of Ag_3PO_4 , a third powder component, into the solid phase or the use of a solution of AgNO_3 as the liquid phase. The objective of this study was to evaluate the physical–chemical and biological properties of such silver-loaded cements and to determine the best candidate for a dental or orthopaedic application.

2 Materials and methods

2.1 Powders synthesis and characterisation

All syntheses were performed in aqueous media (deionised water). Brushite (B), i.e. dicalcium phosphate dihydrate or DCPD ($\text{CaHPO}_4 \cdot 2\text{H}_2\text{O}$), was synthesised by double

decomposition between a calcium nitrate solution ($\text{Ca}(\text{NO}_3)_2 \cdot 4\text{H}_2\text{O}$; 0.37 mol in 600 mL) and ammonium dihydrogen phosphate ($\text{H}_2\text{PO}_4\text{NH}_4$; 0.37 mol in 1.4 L and 20 mL of ammonium hydroxide solution at 20 % w/w). The pH of the mixture was immediately adjusted to ca. 5.5 by the addition of extra ammonium hydroxide solution. The white precipitate was then allowed to mature in solution, without stirring, for 5 h. It was finally filtered and washed with 2 L of water. Vaterite (V), a polymorph of calcium carbonate CaCO_3 , was also synthesised by double decomposition by adding a solution of calcium chloride ($\text{CaCl}_2 \cdot 2\text{H}_2\text{O}$; 0.5 mol in 250 mL) in a solution of sodium carbonate ($\text{Na}_2\text{CO}_3 \cdot 10\text{H}_2\text{O}$; 0.5 mol in 500 mL of deionised water) using a peristaltic pump (12 mL/min). The white precipitate was immediately filtered and washed with 1.5 L of water. After filtration and washing, the precipitates were lyophilised and the powders were stored in a freezer.

Silver orthophosphate Ag_3PO_4 was prepared by double decomposition between silver nitrate (AgNO_3 ; 36 mmol in 200 mL) and disodium hydrogen phosphate (Na_2HPO_4 ; 12 mmol in 300 mL). The yellow precipitate was filtered and washed with 500 mL of water. As Ag_3PO_4 is light sensitive, all the glassware was covered by aluminium foil to keep the solution and powder in darkness during synthesis, drying and storage. Commercial silver nitrate salt (AgNO_3 99.9 %; Alfa Aesar[®]) was purchased and used without further purification.

All the synthesised powders were characterised by transmission Fourier transformed infrared spectroscopy from KBr pellets (FTIR; Perkin-Elmer FTIR 1600 spectrometer), X-ray diffraction (XRD; Inel CPS 120 diffractometer) using a Co anticathode and by scanning electron microscopy (SEM; Leo 435 VP microscope).

2.2 Cement preparation

The reference cement (C-REF cement) was obtained by mixing deionised water as the liquid phase with the solid phase composed of an equal mass of vaterite and brushite. These reactive powders were first homogenised with a pestle in a ceramic mortar.

Silver was introduced into the cement either in the solid phase or in the liquid phase by means of silver salts with different solubilities (Ag_3PO_4 and AgNO_3). Silver-loaded cement pastes were prepared by mixing an appropriate amount of silver phosphate salt (Ag_3PO_4) with the solid phase (C-Ag(S) cement), or by using a silver nitrate (AgNO_3) solution as the liquid phase (C-Ag(L) cement); the amount of silver salt added in the cement formulation is reported in Table 1. In both types of silver-loaded cements prepared (C-Ag(S) and C-Ag(L)), the silver salt was introduced in the cement formulation in order to reach a Ca/Ag atomic ratio of 10.3 (Table 1). For the three cement

Table 1 Composition (weight in g) of the different prepared and studied cements: C-REF, C-Ag(S) and C-Ag(L) cements

Cements	Solid phase (S) (g)			Liquid phase (L) (g)		Weight ratio W/S	Atomic ratios		
	Brushite (B)	Vaterite (V)	Ag ₃ PO ₄	Water (W)	AgNO ₃		Ca/Ag	Ca/P	Ca/C
C-REF	0.50	0.50	–	0.55	–	0.55	–	2.72	1.58
C-Ag(S)	0.45	0.45	0.10	0.55	–	0.55	10.3	2.50	1.58
C-Ag(L)	0.50	0.50	–	0.55	0.13	0.55	10.3	2.72	1.58

compositions (C-REF, C-Ag(S) and C-Ag(L)), the water/solid weight ratio (W/S) was 0.55 (Table 1). After mixing, the wet paste was placed in a water-saturated oven at 37 °C for setting and hardening.

For the cytotoxicity and microbiological tests, pellets of the cements were prepared under the same conditions using silicon rubber moulds (diameter: 10 mm). After setting and drying, the surface of the pellets was polished with fine sand paper (P1200) before γ -ray sterilisation and in vitro tests.

2.3 Cement characterisation

The cements were characterised by the FTIR, XRD and SEM techniques. The setting time of the cement paste was evaluated by the Gillmore needle method (standard ISO 9917-1:2007).

The chemical setting reaction was followed by FTIR spectroscopy. For each composition, eight samples of cement (0.9 ± 0.2 g) were formed from the same initial paste immediately at the end of mixing. They were then placed in an oven at 37 °C in a humid atmosphere for various periods of maturation (0, 1, 2, 3, 4, 7, 24 and 48 h) and then lyophilised in order to remove the water and stop the setting reaction. They were then weighed and analysed by FTIR spectroscopy. The 850–450 cm⁻¹ range of wavenumbers contains several vibration bands characteristic of the different phases involved in cement setting and hardening (Table 2). Significant bands at 525, 603, 617 and 745 cm⁻¹ were carefully chosen in order to evaluate the relative ratios between brushite, apatite and vaterite respectively. The silver orthophosphate phase could not be identified in a relevant way by FTIR spectroscopy due to the superimposition of bands, the very low amount of silver phosphate in the cements and the possible precipitation of AgBr within the KBr pellet. Thus, it was not taken into account for the quantification. During the setting reaction, the solid phase lost about 10 % of its weight (because of CO₂ degassing); we also assumed that the silver phase was not involved in this loss. Some binary and ternary standard samples were prepared by mixing known amounts of brushite, vaterite and a synthetic nanocrystalline carbonated apatite left to mature for 48 h.

Table 2 Assignments of the characteristic absorption bands used to decompose the FTIR spectra in the 850–450 cm⁻¹ domain

Position (cm ⁻¹)	Phases	Attribution
787	B	P–O–H
745	V	ν_2 CO ₃ ²⁻
743	Ap–B	Water libration
664	B	Water libration
615	Ap	Non-apatitic PO ₄ ³⁻
601	Ap	Apatitic PO ₄ ³⁻
577	Ap–B	Apatitic and brushitic PO ₄
560	Ap– Ag	Apatitic and silver orthophosphate PO ₄ ³⁻
533	Ap–B	Non-apatitic and brushitic HPO ₄ ²⁻
524	B	HPO ₄ ²⁻

B brushite, V vaterite, Ap carbonated apatite, Ag Ag₃PO₄

Two domains, i.e. 850–700 and 700–450 cm⁻¹, of the FTIR spectrum of both cements and standards were decomposed into different bands as reported in Table 2 using OriginPro 8.5 software. The baseline was fixed as a straight line between the two minima of each studied domain. An example of decomposition is shown in Fig. 1 for the C-REF cement after 7 h of maturation. The relative areas of the FTIR bands characteristic of each phase involved in the CaCO₃–CaP cements were compared to those of the standards. This allowed for an evaluation of the content of the brushite, vaterite and apatite phases in the studied cement.

2.4 Indirect cytotoxicity study

Cytotoxicity tests are essential before the in vivo evaluation of a new biomaterial. The indirect cytotoxicity evaluation of silver-doped and reference CaCO₃–CaP cement compositions was assessed by an extraction method according to NFEN30993-5 ISO 10993-5 [30].

Human bone marrow stroma cells, obtained from human bone marrow according to Vilamitjana-Amédée et al. [31] with some modifications, were used to test the cytotoxicity of the extracts and cultured in alpha-MEM without ascorbic acid (Invitrogen, France) containing 10 % (v/v) foetal calf serum (FSC, Lonza, France). At passage 2, the cells

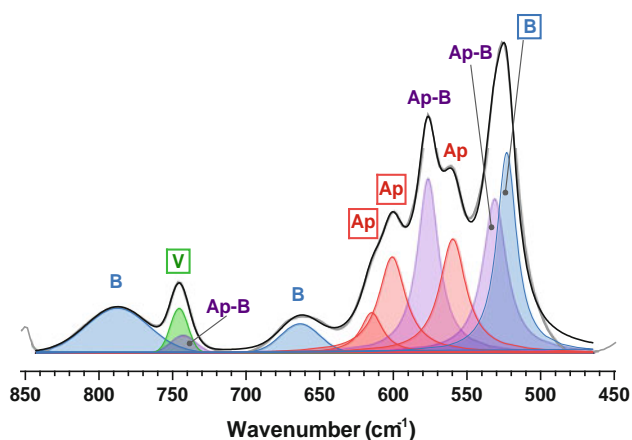


Fig. 1 Example of decomposition of the 850–450 cm^{-1} domain for the cement C-REF after 7 h of maturation. The grey curve corresponds to the experimental FTIR spectrum and the black curve to the sum of the fitted bands. The circled bands are those used for the evaluation of the relative composition between brushite (B), vaterite (V) and apatite (Ap)

were seeded at a density of 40,000 cells/ cm^2 in 96-well microtitre plates (Nunc, Denmark) and the culture was maintained at 37 °C for 96 h after cell plating. At sub-confluency, the medium was replaced by the material extraction vehicle. To obtain extraction vehicles, the hardened cements loaded with silver were sterilised by γ -rays (25 kGy) and then immersed in alpha-MEM medium. The ratio of the sample surface area to the volume of the vehicle was 5 cm^2/mL . Extractions were performed in borosilicate glass tubes at 37 °C for 24 h and this step was repeated five times using the same approach. The extraction liquid was supplemented with 10 % (v/v) FCS. Borosilicate tubes containing identical extraction vehicles with either no material or a solution of phenol at a concentration of 64 g/L (known to be cytotoxic) were processed under the same conditions to provide negative and positive controls, respectively. The medium was replaced by each extract solution supplemented with 10 % (v/v) FCS and the plate was incubated for 24 h at 37 °C. At the end of the extract incubation period, tests were performed: cell viability was assessed by the Neutral Red assay and cell metabolic activity using the MTT assay [32, 33]. The intensity of the colours obtained (red and blue, respectively) is directly proportional to the viability and metabolic activity of the cell population and inversely proportional to the toxicity of the material. Indirect cytotoxicity tests were duplicated for each cement composition. The mean values of absorbance measurements obtained from colorimetric tests and their corresponding standard deviations ($\pm\text{SD}$) were calculated. The results are expressed as a percentage of the negative control (plastic) tested during the same experiment.

2.5 Antibacterial in vitro test

In an attempt to define the effect of silver incorporation, the antibacterial activity was investigated considering the ability of staphylococci to adhere and colonise cement surfaces. *S. aureus* CIP 4.83 and *S. epidermidis* CIP 68.21 (Institute Pasteur Collection, Paris, France) were grown in 24-well microplates containing reference and silver-loaded cement pellets and 2 cm^3 of modified biofilm broth (MBB), as previously described by Khalilzadeh et al. [34]. The model was chosen considering that the composition of MBB and the renewal of the medium promotes adherent but not planktonic cell growth with a biofilm structure. After initial inoculation with 10^2 CFU, the MBB medium was renewed at 2, 4, 6, 20, 24 and 48 h for *S. aureus* and at 6, 20, 24 and 48 h for *S. epidermidis* incubation at 37 °C after two gentle rinses with sterilised distilled water (2 cm^3). Biofilms were grown for 72 h. After the period of growth (72 h), the wells and cement pellets were rinsed and 2 cm^3 of distilled water were added. Adherent bacteria were removed by scraping with a sterile spatula and CFU numeration was performed on the solution. The entire suspension was directly inoculated in trypticase soy agar (Biomérieux, Craaponne, France) or tenfold diluted before adding 100 μL in trypticase soy agar (incubation 48 h at 37 °C). Each experiment was performed three times.

3 Results

3.1 Composition and structure

Figure 2 shows the XRD patterns of the cements after setting and hardening. It appears that a biomimetic poorly crystallised apatite was formed during the setting reaction by the consumption of brushite and vaterite. Nevertheless, some vaterite, initially introduced in excess, remained in the final composition. The addition of silver as Ag_3PO_4 into the solid phase (C-Ag(S) cement) did not affect the final composition: a similar content of apatite and vaterite phases were identified by XRD analysis and silver remained as a distinct crystalline phase (silver orthophosphate) in the cement. Interestingly, similar XRD patterns were obtained for both the C-Ag(S) and C-Ag(L) cements. Thus, it appears that silver orthophosphate, with a very low solubility (1.5310^{-5} g/L at 19.5 °C), precipitated when the silver nitrate solution was added to the cement solid phase. An instantaneous yellow coloration, characteristic of silver orthophosphate, appeared at mixing time t_0 and the XRD data (not shown) confirmed the very fast precipitation of Ag_3PO_4 .

We followed the chemical setting of the different cements by FTIR spectroscopy. The spectra of the three cement

compositions at different maturation times (1, 4 and 48 h) are shown in Fig. 3. We could clearly observe in Fig. 3 that at 1 h and even more at 4 h the decrease in the characteristic band of the brushite phase at 525 cm^{-1} in favour of an increase in apatite characteristic bands at 603 and 617 cm^{-1} : this was significantly higher for C-Ag(L) than for the two other types of cement, indicating faster chemical setting for the C-Ag(L) cement. After 48 h, both silver-loaded cements spectra showed that the brushite characteristic band at 525 cm^{-1} was no longer present, suggesting that this reactive powder was totally consumed, whereas this band was weak but still observable in the reference cement (C-REF) spectrum.

To complete these observations, we performed a semi-quantitative study to evaluate the formation of the apatite phase during cement setting and hardening. Figure 4 shows the evolution of the amount of apatite formed, determined as described in the Materials and Methods section, and its evolution during 48 h of maturation for the three types of

cement tested. It confirms that during the first 8 h, the addition of Ag_3PO_4 in the solid phase did not seem to have a significant impact on the formation of apatite, whereas the increase in the amount of apatite was much faster for C-Ag(L) cement. Between 8 and 24 h, C-Ag(S) caught up to C-Ag(L), so that after 48 h, both cements containing silver were totally set, in terms of the chemical setting reaction, whereas for the C-REF cement, it took a longer time for the setting reaction to reach the same level of apatite content.

Complementarily, the physical setting of the cements was measured using a Gillmore needle apparatus (Table 3). For the C-REF cement, the initial and final setting times were 1 h 15 min and 2 h 15 min, respectively. Despite faster chemical reaction rates, no highly significant differences were observed for the silver-containing cements

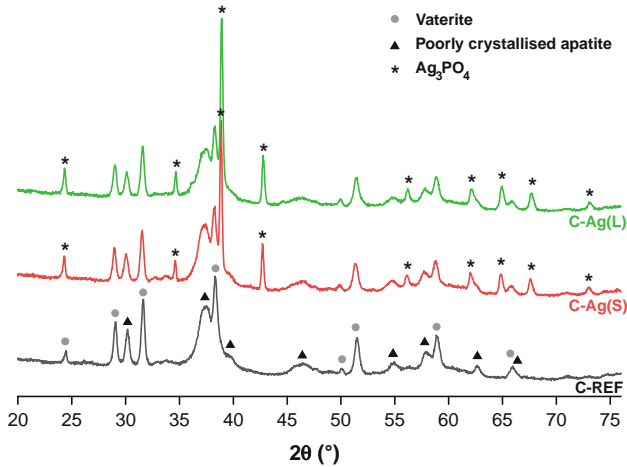


Fig. 2 XRD patterns of the three types of hardened cements: C-REF, C-Ag(S) and C-Ag(L)

Fig. 3 Superimposition of FTIR spectra ($850\text{--}450\text{ cm}^{-1}$ domain) of the three types of cements studied: C-REF, C-Ag(S) and C-Ag(L) after various periods of maturation during setting (1, 4 and 48 h)

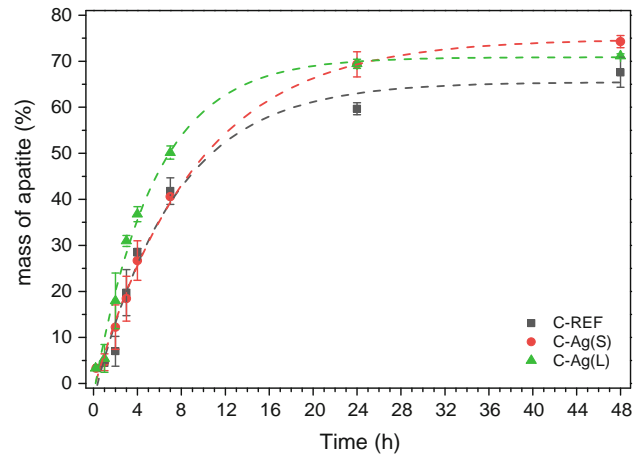
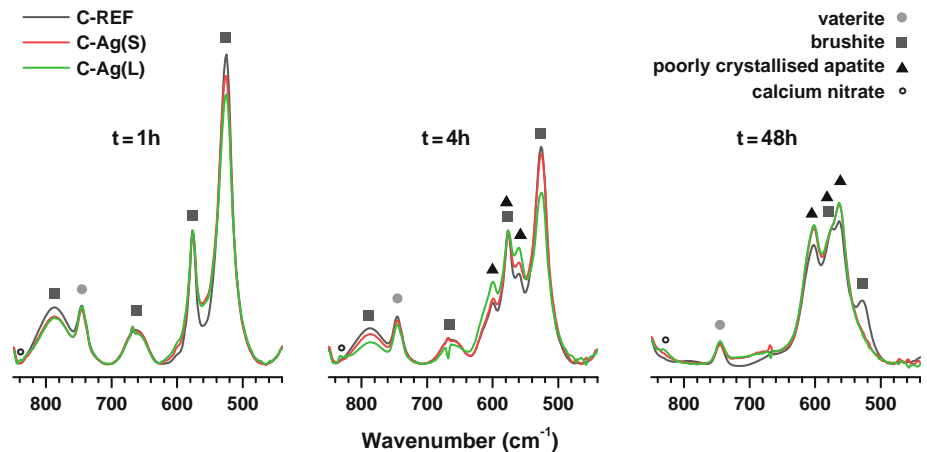


Fig. 4 Evolution of the quantity of apatite formed (as determined by FTIR spectroscopy) within the three types of cement (1 g of cement) during setting. Each curve was fitted by the equation $y = a * \exp(-x/\tau) + y_0$, the main parameters are the following: C-REF: $\tau = 7.2 \pm 1.2\text{ h}^{-1}$, $y_0 = 65.5 \pm 3.3\%$; C-Ag(S): $\tau = 9.2 \pm 0.7\text{ h}^{-1}$, $y_0 = 74.9 \pm 1.7\%$; C-Ag(L): $\tau = 5.5 \pm 0.6\text{ h}^{-1}$, $y_0 = 70.9 \pm 2.2\%$

Table 3 Setting time of the cements measured by the Gillmore needle apparatus

	Initial setting time ^a	Final setting time ^a
C-REF	1 h 15 min	2 h 15 min
C-Ag(S)	1 h 15 min	2 h 00 min
C-Ag(L)	1 h 30 min	2 h 15 min

^a Measurements were performed every 15 min and in triplicate for each type of cement tested. Thus, the uncertainty of the values is ± 15 min

regarding the reference setting time. The introduction of silver as AgNO_3 solution (liquid phase) seemed to slightly delay the initial cement setting time.

Backscatter SEM images of C-Ag(S) and C-Ag(L) cements are presented in Fig. 5. Particles containing silver, which is the heaviest element in the cement compositions tested, appeared much brighter than the calcium phosphate and calcium carbonate phases. In the C-Ag(S) cement, the silver orthophosphate particles (ca. 2 μm) were homogeneously distributed throughout the cement matrix, in relation to the initial homogenisation of the reactive powders before the addition of the liquid phase, whereas in the C-Ag(L) cement, silver phosphate particles were smaller (a few hundred nanometres) and do not appear homogeneously distributed. In addition, we could see that both cements were microporous. Some macropores (>50 μm in diameter) were also present, in particular in the C-Ag(L) cement.

3.2 Biological properties

3.2.1 *In vitro* cytotoxicity tests

Figure 6 shows the evolution of cell viability based on extracts obtained sequentially every 24 h for the C-Ag(S) cement. The extracts from this cement affected the viability and metabolic activity of cells during the first 24 h only, as evidenced by the results obtained with both the MTT and NR assays. For the following extractions, we found a progressive increase in cell viability, but no significant variation in their metabolic activity, which suggests that with successive extractions, the C-Ag(S) cement remained non-cytotoxic, especially after the fifth extraction of the functionalised cement. Similar results were obtained for the C-Ag(L) cement (data not shown).

3.2.2 Antibacterial *in vitro* tests

Table 4 presents the CFU enumeration per cement pellet after 72 h of incubation with *S. aureus* CIP 4.83 and *S. epidermidis* CIP 68.21.

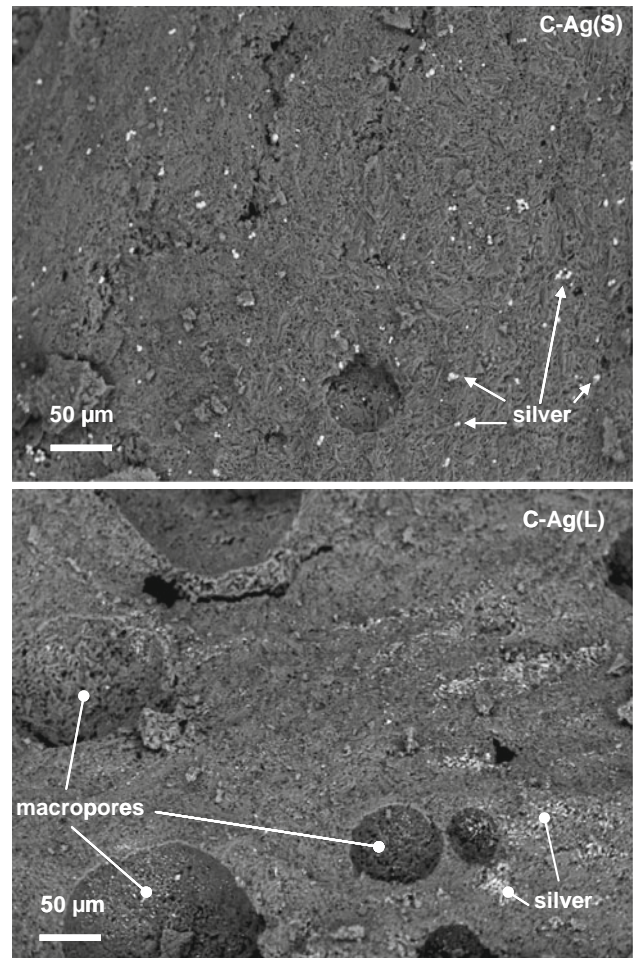


Fig. 5 SEM images (backscattered electrons) of C-Ag(S) and C-Ag(L) cements showing the distribution of silver (bright dots) into both types of cement

For both strains of staphylococci tested, which are the main species involved in bone-implant infections, we could observe a dramatically decrease in bacterial numeration (anti-adhesion and anti-biofilm formation effect) since 0 CFU of adherent bacteria were obtained for the C-Ag(S) cement ($P < 0.001$) whereas values with the reference cement (control) were similar to those obtained directly in wells with no cement. Log reductions were higher than 6 in all the assays. Similar results were obtained for the C-Ag(L) cement (data not presented).

4 Discussion

4.1 Composition and setting of silver-loaded cements

In a previous study, it was shown that the setting of the calcium carbonate–calcium phosphate mixed cement

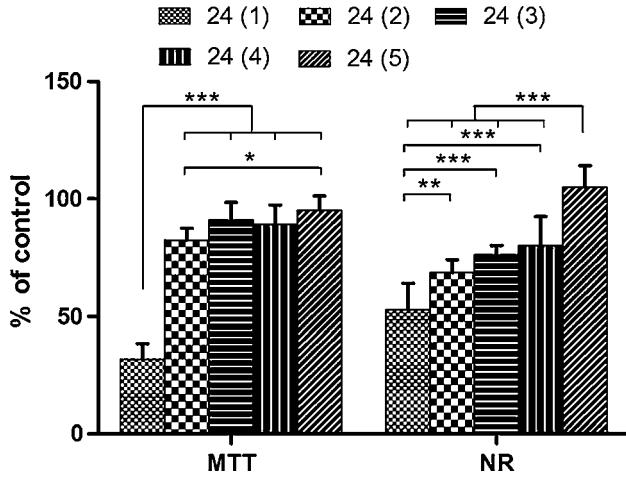
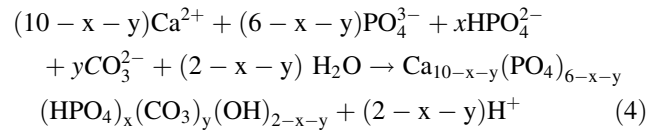
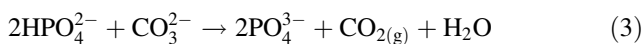
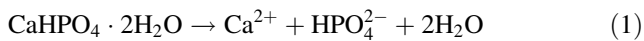


Fig. 6 Indirect cytotoxicity evaluation. Cell viability (neutral red (NR) assay) and cell metabolic activity (MTT assay) of cells incubated for 24 h at 37 °C in five different extracts obtained by successive extractions. Five extractions of C-Ag(S) cement in the vehicle medium were performed every 24 h and are designated in the figure as 24 (1) to 24 (5). Results are expressed as % of the negative control material (plastic)

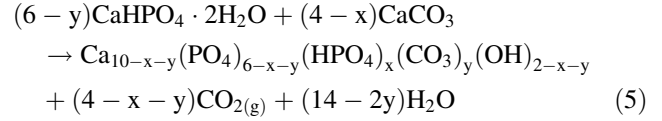
Table 4 Log CFU of adherent bacteria (*S. aureus* CIP 4.83 and *S. epidermidis* CIP 68.21) after 72 h of incubation with the reference (control) and silver-loaded (C-Ag(S)) cement pellets (mean \pm SD; $n = 3$)

	Reference cement	C-Ag(S) cement
<i>S. aureus</i>	6.98 \pm 0.12	<3
P value (C vs. E)		<0.001
<i>S. epidermidis</i>	6.86 \pm 0.08	<3
P value (C vs. E)		<0.001

(C-REF) leads to the formation of a biomimetic nanocrystalline apatite by a dissolution-precipitation reaction [35]. In this nanocrystalline apatite, some of the PO_4^{3-} anions can be substituted by the divalent anions HPO_4^{2-} and CO_3^{2-} also present in the self-setting system, thus creating calcium and hydroxyl vacancies to maintain the electroneutrality of the solid. According to the literature, and considering our self-setting system, we can assume that the general chemical formula of the apatite formed is $\text{Ca}_{10-(x+y)}(\text{PO}_4)_{6-(x+y)}(\text{HPO}_4)_x(\text{CO}_3)_y(\text{OH})_{2-(x+y)}$ with $0 \leq x + y \leq 2$ [36]. Thus, the main chemical reactions involved in the studied cement (dissolution of brushite and vaterite (Eqs. 1, 2), the reaction between hydrogenophosphate and carbonate ions (Eq. 3) and the reprecipitation of apatite (Eq. 4)) are represented by the following equations:



According to these four equations, the global system can be modelled as follows:



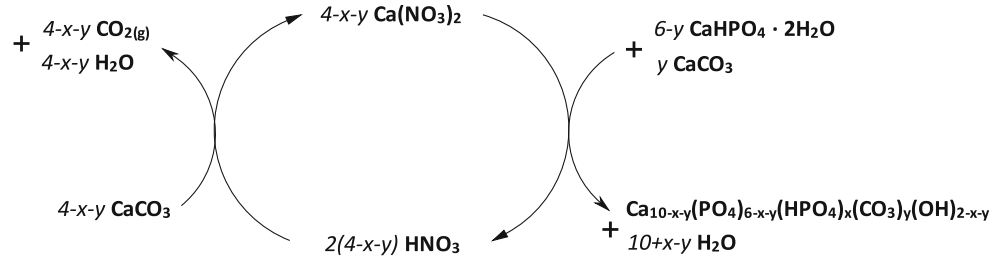
The formation of carbon dioxide (Eqs. 3, 5) can explain the presence of macropores observed within the set cement (Fig. 5).

In the present study, we showed that the introduction of a silver salt into the cement composition did not change the reaction mechanism: brushite dissolved and reacted with some vaterite to form an apatite phase (Fig. 2). Nevertheless, FTIR spectroscopy semi-quantitative analysis revealed a slight change in the setting kinetics, as the setting reaction (chemical setting) rate appeared faster for the cements containing silver (Fig. 2), whereas the setting time (physical setting) was unchanged for C-Ag(S) and slightly longer for C-Ag(L) (Table 3). It shall be recalled that the physical setting time, corresponding to paste hardening, although related to the chemical reactions involved, does not superimpose with the advancement of these chemical reactions. We discuss hereafter the chemical and physical processes leading to the setting of these cements.

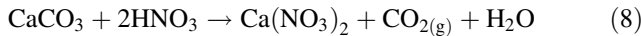
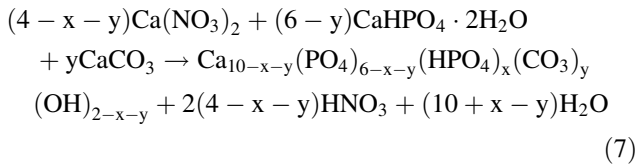
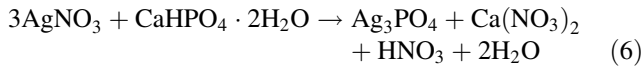
As mentioned before, Ag_3PO_4 , introduced in the C-Ag(S) cement or immediately formed in the C-Ag(L) cement, has a low solubility, much lower, comparatively, than that of brushite and vaterite. Although it may not induce a major change in the dissolution-precipitation reactions, it could have an impact on ion equilibrium involved in these processes.

In the case of the C-Ag(L) cement, the precipitation of Ag_3PO_4 observed immediately after the addition of silver nitrate solution to the cement reactive powders mixture induced, on the one hand, the beginning of the consumption of phosphate ions from the brushite, consistent with the earlier decrease in the phosphate band after 1 and 4 h (Fig. 2) and, on the other hand, an acidification of the medium (Eq. 6). Since $\text{Ca}(\text{NO}_3)_2$ is highly soluble (1.44×10^3 g/L at 25 °C), calcium ions are more readily available to form some apatitic nuclei than in the C-REF cement (Eq. 7). The acidification of the medium can also favour the dissolution of the reactants, particularly acting on vaterite by an acid-base reaction (Eq. 8), which leads to the release of carbon dioxide and the regeneration of $\text{Ca}(\text{NO}_3)_2$ which was initially involved in the precipitation of apatite. Given Eqs. (7) and (8), it appears that $\text{Ca}(\text{NO}_3)_2$ could play the role of a catalyst in the self-setting system,

Fig. 7 Schematic representation of the catalytic role of $\text{Ca}(\text{NO}_3)_2$ in apatite precipitation within the C-Ag(L) cement



as described in Fig. 7, until the complete dissolution of brushite, the limiting reactant. Its involvement could explain the faster precipitation of apatite observed by FTIR spectroscopy (Fig. 3).



In the case of the C-Ag(S) cement, the low solubility of Ag_3PO_4 introduced directly to the reactive powder mixture (solid phase) made it a “spectator” phase at the beginning of the setting process, in agreement with the absence of a significant influence noticed on chemical (Fig. 2) and physical (Table 3) setting. However, during the setting reaction, apatite was formed, hence inducing an acidification of the medium (Eq. (4)). This acidification might transiently favour the dissolution of silver phosphate. On the XRD pattern, the relative intensity of Ag_3PO_4 appeared to decrease during setting (data not shown), and no additional phase was identified. An increased concentration of phosphate ions will favour the formation of apatite. On the other hand, although no shift of the XRD peaks can be clearly observed, some Ag^+ ions could probably be incorporated into the cationic lattice of the apatite. This may also accelerate the precipitation process, as observed after about 10 h of maturation (Fig. 4). Vandecandelaere studied the conditions of formation of silver-doped nanocrystalline apatites and showed that neutral and alkaline conditions allowed for obtaining silver-doped nanocrystalline apatites (more Ag incorporated at neutral pH), whereas acidic conditions favoured the precipitation of silver phosphate [37]. In addition, this study revealed a slight increase in apatite crystal length when silver was incorporated into the nanocrystalline apatite structure. However, no inhibitory or promoter effect of the presence of silver on nanocrystalline apatite crystal growth has been demonstrated.

The setting and hardening of cements is a complex phenomenon, and is not always correlated with the chemical reaction rate involved in the setting process: while during the first 12 h of cement maturation, apatite was formed more rapidly in the C-Ag(L) cement than in the C-Ag(S) or C-REF cements (Fig. 4), hardening took slightly longer (higher initial setting time, Table 3). The more acidic initial medium and/or the presence of silver might lead to smaller crystallites of apatite or to a greater disorder of the structure, which could explain the slight delay in the physical entanglement of particles and thus of hardening.

The backscatter mode SEM images showed two major differences in C-Ag(S) and C-Ag(L) cement microstructure: the size of the silver-rich particles (2 μm and a few hundred nanometres respectively) and their distribution. These two key parameters could have an impact on the antibacterial activity of the cement. Homogeneity of the distribution of silver is of course necessary in order to control the local concentration of the antibacterial agent in the material. It would be necessary to optimise the mixing time and processing of the paste of the C-Ag(L) cement in order to better homogenise the distribution of the silver phosphate formed in situ. The size of the particles can be discussed in terms of solubility: smaller particles will probably have a higher rate of solubilisation and thus faster kinetics of Ag^+ release. Our objective was to obtain a preventive effect of silver and to avoid any bacterial growth on the material. For this application, it would be better to maintain a sufficient concentration of silver on the surface of the materials, avoiding rapid release. Considering these two aspects, and given that there were no major differences in the physico-chemical properties between the two silver-loaded cements, C-Ag(S) appears to be better candidate as bone substitute, as it did not introduce any other counter ions such as nitrate in the cement composition.

4.2 Biological properties of silver-loaded cements

The preliminary study on the in vitro biological properties showed that silver-loaded CaCO_3 -CaP cements had

antibacterial properties (anti-adhesion and anti-biofilm formation) without cytotoxic effects on human bone marrow stromal cells after several washings of the cements, even if a high dose of Ag was incorporated within cement (Ag/Ca atomic ratio equal to 9.7 %).

The significant decrease in cell viability and metabolic activity observed for cells in contact with the first extract (first 24 h) suggests that a burst release of Ag should occur during the equilibration of the C-Ag(S) cement with the medium (alpha-MEM) at a high dose, such that cell viability and metabolic activity were affected. However, for the following extracts, cell viability as well metabolic activity were restored, suggesting that with the equilibration of the cements in alpha-MEM, HBMS cells are able to grow and to proliferate in contact with the extracts. Successive washings of CaP cements or ceramics are needed for equilibrating the materials before cell seeding or metabolic activity test. Considering the dynamic renewal of biological fluids in vivo and the homogeneous distribution of silver within the C-Ag(S) cement observed by microscopy (Fig. 4), we can expect good cytocompatibility of this cement even in the early period after implantation.

The introduction of silver as an antibacterial agent in hydroxyapatite and brushite bone cements has been reported by Ewald et al. [29], who used silver-doped TCP (α - or β -TCP, respectively) as reactive powders to prepare both cements. They showed that silver-doped brushite cement (Ag/Ca = 0.6 %) was the most efficient cement with regards to two strains of staphylococci, but this cement was also cytotoxic to osteoblasts in which activity began to recover only after 7 days of culture. This behaviour may be related to the high solubility of brushite under biological conditions, which should in turn contribute to the release of a high amount of silver into the cell culture medium. In addition, the probable hydrolysis of brushite into apatite in vivo may generate locally an acidic pH favouring Ag^+ release. However, the possibility of precipitating a poor soluble silver phosphate after brushite hydrolysis was not considered by the authors although it may explain the recovery of cell activity after 7 days.

The dose of silver incorporated in the CaCO_3 -CaP cements was high, but this can be optimised with regards to the antibacterial properties and cytocompatibility of the biomaterial. In addition, the route of introduction proposed in the present study (silver salt added as a separate ingredient within the solid or liquid phase) has the advantage of allowing the dose of antibacterial agent to be adapted during surgery and then delivered locally depending on the application and the patient. Biological activity (antibacterial and cytotoxicity) of silver associated or not to hydroxyapatite has been earlier described and explored

[15, 20, 21]. The presented assays had to be considered as preliminary results to check the maintenance of known efficiency when silver is incorporated in calcium carbonate-calcium phosphate bone cement. Antimicrobial assays were performed in conditions allowing biofilm formation but not planktonic growth, because such adherent bacteria are significantly more resistant to immune system and antibiotics treatments. In addition, these conditions are more representative of the pathologic situation since biofilm formation is required to induce chronic bones infections [38]. Pellets including the tested silver amount displayed some strong anti-adhesive and/or anti-biofilm formation exerted by silver associated with a CaCO_3 -CaP cement on *S. aureus* and *S. epidermidis*, two major bone pathogens [39, 40]. Our protocol allowed us to get a detection limit as low as we were able to assess no CFU from the cement surface after 72 h of incubation, whereas more than 10^6 CFU were detected for control cement pellets. The observed effects for such components can be expected to be reproducible in long term in vivo conditions, because of the total adhesion and biofilm formation inhibition, even after 3 days of contact with an initial inoculum of 10^2 CFU/cm², which can be considered as an in vivo worth case. A thorough study focusing on the release properties (Ag release) and on the effect of Ag dose on the biological properties of these cements is in progress and will be presented in another paper.

Local delivery of the antibacterial agent presents an alternative to the use of high and daily doses delivered systemically and the toxicity or side effects associated with this mode of drug administration.

5 Conclusion

This study contributes to understanding the complex chemical reactions involved in silver-doped CaCO_3 -CaP cement paste setting, and we proposed a chemical scheme involving calcium nitrate as a catalytic agent in apatite precipitation during C-Ag(L) cement setting. In vitro biological tests revealed the antibacterial properties of these cements and their non-cytotoxicity after washing, making silver-doped CaCO_3 -CaP cement a promising bone substitute material to reduce implant-associated infections. Interestingly, we can take advantage of the two routes of introduction of silver as a separate ingredient in the cement formulation to adapt the dose of antibacterial agent up to the final step, i.e. during surgery.

Acknowledgments The authors thank the Agence Nationale de la Recherche (ANR-TecSan 2009 program) for supporting this research (BIOSINJECT-ANR-09-TECS-004 project).

References

1. Brown WE, Chow LC. A new calcium phosphate setting cement. *J Dent Res.* 1983;62:672.
2. Bohner M. Design of ceramic-based cements and putties for bone graft substitution. *Eur Cells Mater.* 2010;20:1–12.
3. Sugawara A, Asaoka K, Ding S-J. Calcium phosphate-based cements: clinical needs and recent progress. *J Mater Chem B.* 2013;1:1081–9.
4. Combes C, Bareille R, Rey C. Calcium carbonate-calcium phosphate mixed cement compositions for bone reconstruction. *J Biomed Mater Res Part A.* 2006;79:318–28.
5. Ginebra M-P, Canal C, Espanol M, Pastorino D, Montufar EB. Calcium phosphate cements as drug delivery materials. *Adv Drug Deliv Rev.* 2012;64:1090–110.
6. Joosten U, Joist A, Frebel T, Brandt B, Diederichs S, Von Eiff C. Evaluation of an in situ setting injectable calcium phosphate as a new carrier material for gentamicin in the treatment of chronic osteomyelitis: studies in vitro and in vivo. *Biomaterials.* 2004;25:4287–95.
7. Liu WC, Wong CT, Fong MK, Cheung WS, Kao RYT, Luk KDK, et al. Gentamicin-loaded strontium-containing hydroxyapatite bioactive bone cement—an efficient bioactive antibiotic drug delivery system. *J Biomed Mater Res B Appl Biomater.* 2010;95:397–406.
8. Hesaraki S, Nemati R. Cephalixin-loaded injectable macroporous calcium phosphate bone cement. *J Biomed Mater Res B Appl Biomater.* 2009;89:342–52.
9. Sasaki T, Ishibashi Y, Katano H, Nagumo A, Toh S. In vitro elution of vancomycin from calcium phosphate cement. *J Arthroplasty.* 2005;20:1055–9.
10. Jiang P-J, Patel S, Gbureck U, Caley R, Grover LM. Comparing the efficacy of three bioceramic matrices for the release of vancomycin hydrochloride. *J Biomed Mater Res B Appl Biomater.* 2010;93:51–8.
11. Serraj S, Michăilescu P, Margerit J, Bernard B, Boudeville P. Study of a hydraulic calcium phosphate cement for dental applications. *J Mater Sci Mater Med.* 2002;13:125–31.
12. Michăilescu P, Kouassi M, El Briak H, Armynot A, Boudeville P. Antimicrobial activity and tightness of a DCPD–CaO-based hydraulic calcium phosphate cement for root canal filling. *J Biomed Mater Res B Appl Biomater.* 2005;74:760–7.
13. Gbureck U, Knappe O, Grover LM, Barralet JE. Antimicrobial potency of alkali ion substituted calcium phosphate cements. *Biomaterials.* 2005;26:6880–6.
14. Lansdown ABG. A pharmacological and toxicological profile of silver as an antimicrobial agent in medical devices. *Adv Pharmacol Sci.* 2010;2010:1–16.
15. Feng QL, Wu J, Chen GQ, Cui FZ, Kim TN, Kim JO. A mechanistic study of the antibacterial effect of silver ions on *Escherichia coli* and *Staphylococcus aureus*. *J Biomed Mater Res.* 2000;52:662–8.
16. Berbari EF, Hanssen AD, Duffy MC, Steckelberg JM, Ilstrup DM, Harmsen WS, et al. Risk factors for prosthetic joint infection: case-control study. *Clin Infect Dis.* 1998;27:1247–54.
17. Lansdown ABG. Silver in healthcare: its antimicrobial efficacy and safety in use. Cambridge: Royal Society of Chemistry; 2010.
18. Kim TN, Feng QL, Kim JO, Wu J, Wang H, Chen GC, et al. Antimicrobial effects of metal ions (Ag^+ , Cu^{2+} , Zn^{2+}) in hydroxyapatite. *J Mater Sci Mater Med.* 1998;9:129–34.
19. Singh B, Dubey AK, Kumar S, Saha N, Basu B, Gupta R. In vitro biocompatibility and antimicrobial activity of wet chemically prepared $\text{Ca}_{10-x}\text{Ag}_x(\text{PO}_4)_6(\text{OH})_2$ ($0.0 \leq x \leq 0.5$) hydroxyapatites. *Mater Sci Eng C.* 2011;31:1320–9.
20. Chen W, Liu Y, Courtney HS, Bettenga M, Agrawal CM, Bumgardner JD, et al. In vitro anti-bacterial and biological properties of magnetron co-sputtered silver-containing hydroxyapatite coating. *Biomaterials.* 2006;27:5512–7.
21. Ando Y, Miyamoto H, Noda I, Sakurai N, Akiyama T, Yonekura Y, et al. Calcium phosphate coating containing silver shows high antibacterial activity and low cytotoxicity and inhibits bacterial adhesion. *Mater Sci Eng C.* 2010;30:175–80.
22. Ghafari Nazari A, Tahari A, Moztafzadeh F, Mozafari M, Bahrololoom ME. Ion exchange behaviour of silver-doped apatite micro- and nanoparticles as antibacterial biomaterial. *Micro Nano Lett.* 2011;6:713–7.
23. Shirkhazadeh M, Azadegan M, Liu GQ. Bioactive delivery systems for the slow release of antibiotics: incorporation of Ag^+ ions into micro-porous hydroxyapatite coatings. *Mater Lett.* 1995;24:7–12.
24. Lee JS, Murphy WL. Functionalizing calcium phosphate biomaterials with antibacterial silver particles. *Adv Mater.* 2013; 25:1173–9.
25. Venkateswarlu K, Rameshbabu N, Chandra Bose A, Muthupandi V, Subramanian S, MubarakAli D, et al. Fabrication of corrosion resistant, bioactive and antibacterial silver substituted hydroxyapatite/titania composite coating on Cp Ti. *Ceram Int.* 2012; 38:731–40.
26. Lim, PN, Teo EY, Ho B, Tay BY, Thian ES. Effect of silver content on the antibacterial and bioactive properties of silver-substituted hydroxyapatite. *J Biomed Mater Res Part A.* 2013; 101:2456–64.
27. Spadaro J, Webster D, Becker R. Silver polymethyl methacrylate antibacterial bone cement. *Clin Orthop Relat Res.* 1979;143: 266–70.
28. Alt V, Bechert T, Steinrücke P, Wagener M, Seidel P, Dingeldein E, et al. An in vitro assessment of the antibacterial properties and cytotoxicity of nanoparticulate silver bone cement. *Biomaterials.* 2004;25:4383–91.
29. Ewald A, Hösel D, Patel S, Grover LM, Barralet JE, Gbureck U. Silver-doped calcium phosphate cements with antimicrobial activity. *Acta Biomater.* 2011;7:4064–70.
30. Evaluation biologique des dispositifs médicaux. Partie 5: Essais concernant la cytotoxicité: Méthodes in vitro. AFNOR NF EN 30993-5-ISO 10993-5 1994.
31. Vilamitjana-Amédée J, Bareille R, Rouais F, Caplan AI, Harmand MF. Human bone marrow stromal cells express an osteoblastic phenotype in culture. *In Vitro Cell Dev Biol Anim.* 1993;29:699–707.
32. Parish CR, Müllbacher A. Automated colorimetric assay for T cell cytotoxicity. *J Immunol Methods.* 1983;58:225–37.
33. Mosmann T. Rapid colorimetric assay for cellular growth and survival: application to proliferation and cytotoxicity assays. *J Immunol Methods.* 1983;65:55–63.
34. Khalilzadeh P, Lajoie B, El Hage S, Furiga A, Baziard G, Berge M, et al. Growth inhibition of adherent *Pseudomonas aeruginosa* by an *N*-butanoyl-L-homoserine lactone analog. *Can J Microbiol.* 2010;56:317–25.
35. Combes C, Bareille R, Rey C. Calcium carbonate-calcium phosphate mixed cement compositions for bone reconstruction. *J Biomed Mater Res Part A.* 2006;79A:318–28.
36. Eichert D, Drouet C, Sfihi H, Rey C, Combes C. Nanocrystalline apatite-based biomaterials: synthesis, processing and characterization. In: Kendall JB, editor. *Biomaterials research advances*, New York: Nova Science Publishers; 2007. pp. 93–143.
37. Vandecandelaere N. Ph.D. Thesis. Élaboration et caractérisation de biomatériaux osseux innovants à base d'apatites phospho-calciques

dopées. Université de Toulouse, Institut National Polytechnique de Toulouse; 2012.

38. Palmer M, Costerton W, Sewecke J, Altman D. Molecular techniques to detect biofilm bacteria in long bone nonunion: a case report. *Clin Orthop Relat Res.* 2011;469:3037–42.
39. Ciampolini J, Harding K. Pathophysiology of chronic bacterial osteomyelitis. Why do antibiotics fail so often? *Postgrad Med J.* 2000;76:479–83.
40. Carek PJ, Dickerson LM, Sack JL. Diagnosis and management of osteomyelitis. *Am Fam Physician.* 2001;63:2413–21.